

# A Motion Tracking Method for the Modeling and Simulation of Human Movement in 3D

Ajay Seth

Department of Biomedical Engineering,  
The University of Texas at Austin  
Austin, USA  
aseth@mail.utexas.edu

**Abstract**—Interest in computer models of the human musculoskeletal system is increasing amongst clinicians and movement scientists as tools to analyze muscle and joint function in ways that are both non-invasive and inexpensive. Quantifying internal loads resulting from muscles and external forces is necessary to understand and treat movement pathologies. Current simulation methods, however, fall short of accurately reproducing observed human performance when compared to observations made during movement experiments. It is a minimal requirement that models closely reproduce external observations before considering them to answer questions about severity of a disorder and possible treatments. Given this underlying requirement, a dynamical motion-tracking method was developed to leverage experimental observations directly to guide forward simulations and provide simulations that are more accurate. In the present study, we demonstrate how tracking can provide joint-moment information that produce accurate forward simulations in minutes using a detailed 23 degree-of-freedom human model and 3D motion-capture data.

**Keywords**—*musculoskeletal modeling; dynamic optimization; jumping; forward dynamics; inverse dynamics*

## I. INTRODUCTION

The accuracy of inverse dynamics is important for many human performance analyses and is the basis for several methods that estimate individual muscle forces. For example, static optimization/decomposition [1], the “method of computed muscle forces” [2], and EMG based [3] methods all require net moments to estimate individual muscle contributions. However, muscular moments from inverse dynamics are inaccurate if they fail to drive a skeletal model in a likely reproduction of the observed movement being analyzed. Inaccuracies do not only arise from noisy position data but by the fact that inverse dynamics performed at discrete points in time often have insufficient control signal dimensionality [4]. Furthermore, applying observed ground-reaction forces (GRFs) directly to a model neglects differences between human and model dynamics and these discrepancies accumulate into large errors in a forward simulation.

Computing joint moments that are stabilized by error-feedback with respect to kinematics has been shown to significantly improve simulation accuracy. Specifically, the method of computed torques [5] has been applied successfully to generate representative forward simulations in models without ground contact dynamics ([6] and [2]). In locomotion,

however, ground contact dynamics play a critical role in total body dynamics, and it is, in fact, the ground reaction force that enables locomotion. Therefore, knowing how contact reacts to muscle moments and body position are essential to understanding how locomotion is controlled. Unfortunately, foot and/or pelvis kinematics necessary to evaluate the forces generated by passive contact models (i.e. [7]) cannot be experimentally measured with sufficient accuracy. Therefore, a method of tracking more reliable GRFs directly is required to reduce the reliance on less accurate kinematics. We have demonstrated using simulated motion-capture data, that GRF tracking could reduce errors introduced by noise-contaminated kinematics [8]. In the present study, we use skeletal motion-tracking to analyze maximal height jumping in 3D using spatial motion-capture data.

The objectives of this study are: 1) to present a motion tracking method for simulating human behavior given skeletal multibody and contact dynamics in 3D; 2) apply the tracking method with experimental data to simulate the highly explosive task of maximum height jumping; and 3) to discuss the results of the motion-tracking method and its implications on human movement modeling and simulation.

## II. METHODOLOGY

### A. Experimental Data

The experimental data used to track the human performance of maximal height jumping was obtained from [7]. In summary, data was collected from five male subjects performing a maximum-height jump, which included the positions of markers affixed to the legs and torso in addition to force-plate data upon which the subject performed the jump (Fig 1A). Spatial marker positions were collected at 60Hz and used to determine the orientation of the segments in 3D from which the joint trajectories for a 23 degree-of-freedom (dof) of model (Fig 1B) were determined. GRFs and center-of-pressure (COP) data were collected at 1000Hz from a single force-plate. The kinematics and GRFs were low-pass filtered at 10Hz and 50Hz, respectively.

### B. Human Skeletal and Contact Dynamics

The 23-dof multibody dynamics model including that back at L4-L5, pelvis and legs (2-thighs, shanks, hindfeet and toes) (Fig 1B) as well as contact model (Fig. 1B) were adapted from

[7] and used to generate forward simulations of vertical jumping. The model simulations produce kinematics (joint trajectories) and ground contact forces with COP coordinates under each foot that are determined by nonlinear spring-damper elements on the bottom of the feet (Fig. 1C).

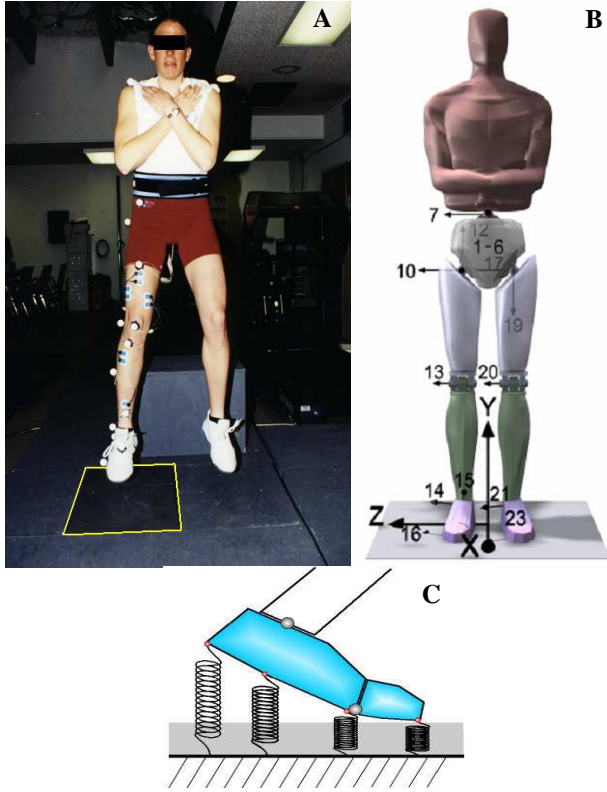


Figure 1. Subject instrumentation (A), multibody jumping model [7] (B) and contact model (C)

Several, modifications to the original contact model described by [7] were necessary to make the model more representative of the actual ground interaction. Mainly, residual forces had to be eliminated to replicate the release (take-off). When the ratio of the net horizontal force (in the ground plane) to the total vertical force exceeded the coefficient of friction, spring constants were determined such that they resulted in zero horizontal forces rather than the frictional limit force.

### C. Motion-Tracking

A skeletal motion-tracking algorithm (Fig. 2), as described by Seth and Pandy [8], was used to determine muscular moments (torques) to actuate the jumping model. In summary, the motion-tracking controller was implemented by applying feedback linearization (FBL) [9] to continuously linearize the skeletal (link-segment) and contact (nonlinear spring-damper) dynamics. In turn, the linearized system was governed by a new set of controls,  $v$ . These were the tracking controls, which were determined according to the linear feedback error between skeletal model outputs,  $(\Theta, s)$ , and their experimental counterparts,  $(\hat{\Theta}, \hat{s})$ . Accordingly, the FBL control law was employed to determine the joint moments (torques),  $\tau$ , required to actuate the nonlinear plant (skeletal model).

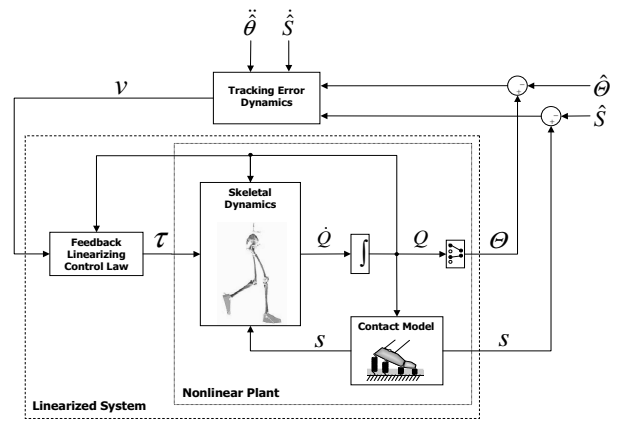


Figure 2. Overview of motion tracking algorithm

The equations of motion for the multi-body (skeletal) dynamics can be written as:

$$\ddot{q} = M^{-1}[\mathfrak{S}(q, \dot{q}) + S(q, \dot{q}) + T\tau] \quad (1)$$

where the generalized coordinates,  $q = [\rho_{1-6}, \omega_{7-23}]^T$ , are the 6-dofs of the pelvis in free-space and the remaining 17 joint angles of the model (Fig 1B);  $M$  is the system mass matrix;  $\mathfrak{S}$  is the set of generalized forces due to gravity, centripetal and Coriolis effects;  $S$  represents the nonlinear spring dynamics used to model foot contact with the ground; and  $T$  is the coefficient matrix relating 17 applied joint torques,  $\tau$ , to the 23 generalized coordinates. In first-order form, Eq. (1) becomes:

$$\dot{Q} = F(Q) + G(Q) \cdot \tau \quad (2a)$$

$$y = [\theta, s]^T \quad (2b)$$

where  $Q = [q, \dot{q}]^T$ ;  $F$  includes the generalized velocities and generalized forces,  $\mathfrak{S}$ , and contact forces,  $S$ ; and  $G = [0_{23 \times 17}, T]^T$ . The multibody equations of motion were generated using SD/Fast<sup>TM</sup>. The output,  $y$ , contains output kinematics,  $\theta$ , which may be all, a subset, or any function of  $q$  (i.e. coordinates 1-23, Fig. 1B); and contact model outputs,  $s = [S_v, S_y, S_z, cop_x, cop_z]^T$ , containing the resultant (combined right and left sides) fore-aft, vertical, and medio-lateral components of the ground contact force as well as the fore-aft and medio-lateral coordinates of the center-of-pressure, respectively.

To determine the FBL control law we differentiate the outputs until the torques,  $\tau$ , are explicitly obtained:

$$\ddot{y}_\theta = \frac{\partial}{\partial Q} \left( \frac{\partial \theta}{\partial Q} \cdot F \right) \cdot F + \frac{\partial}{\partial Q} \left( \frac{\partial \theta}{\partial Q} \cdot F \right) \cdot G \cdot \tau \quad (3a)$$

$$\ddot{y}_s = \frac{\partial s}{\partial Q} \cdot F + \frac{\partial s}{\partial Q} \cdot G \cdot \tau \quad (3b)$$

Introducing the control vector,  $v = [\ddot{y}_\theta, \ddot{y}_s]^T$ , and solving for the torques, yields the FBL control law:

$$\tau = \left[ \begin{array}{c} \frac{\partial}{\partial Q} \left( \frac{\partial \theta}{\partial Q} \cdot F \right) \\ \frac{\partial}{\partial s} \left( \frac{\partial \theta}{\partial Q} \cdot F \right) \end{array} \right]^{-1} \cdot G \left\{ v - \left[ \begin{array}{c} \frac{\partial}{\partial Q} \left( \frac{\partial \theta}{\partial Q} \cdot F \right) \\ \frac{\partial}{\partial s} \left( \frac{\partial \theta}{\partial Q} \cdot F \right) \end{array} \right] \cdot F \right\} \quad (4)$$

that provides the input torques,  $\tau$ , to the nonlinear plant as a function of the new control parameter,  $v$ , which is evaluated by the linear tracker:

$$v = \left\{ \begin{array}{c} \ddot{\theta} - 2\lambda_{\theta}(\dot{\theta} - \dot{\hat{\theta}}) - \lambda_{\theta}^2(\theta - \hat{\theta}) \\ \dot{\hat{S}} - \lambda_s(s - \hat{S}) \end{array} \right\} \quad (5)$$

as a function of given reference signals,  $\hat{\theta}$  and  $\hat{S}$ .

Gains for the motion-tracking controller were determined by a conventional ‘‘rule-of-thumb’’ that poles of a controller should be much (i.e. 5 $\times$ ) faster than the signals being tracked (i.e.  $\lambda_{\theta}=50$  and  $\lambda_s=250$ ). Doubling and then quadrupling  $\lambda_s$  further improved GRF tracking. The inverse in (4) was determined in a least-squares sense [10] with weightings for errors associated with individual outputs ( $y$ ) initially assigned equal weightings. The exceptions were the ankle and toe angles, which were anticipated to be less accurate than other measurements primarily because the experimental orientations of the foot and toes are more error prone due to the proximity of the foot markers compared to those of the shank, thigh or HAT. Gains were subsequently adjusted to arrive at the values in Table 1.

TABLE I. LSQ OUTPUT ( $y$ ) TRACKER WEIGHTINGS ( $W$ )

$y$	$W$	$Y$	$W$	$y$	$W$	$y$	$W$
$q_1$	2	$q_7$	100	$q_{13} / q_{20}$	100	$s_1$	50
$q_2$	2	$q_8$	10	$q_{14} / q_{21}$	2	$s_2$	100
$q_3$	1	$q_9$	10	$q_{15} / q_{22}$	1	$s_3$	25
$q_4$	10	$q_{10} / q_{17}$	100	$q_{16} / q_{23}$	0.5	$s_4$	10
$q_5$	10	$q_{11} / q_{18}$	10			$s_5$	10
$q_6$	100	$q_{12} / q_{19}$	10				

a. Tracking outputs are all coordinates,  $q$ , and contact model outputs,  $s$ .

### III. RESULTS

The motion-tracking method generated a forward dynamics simulation of vertical jumping that followed the experimental values in just under 6 min. The joint angles produced by the model correspond well with the experimental trajectories, especially for back extension, hip flexion, and knee extension angles (Fig. 3). Larger discrepancies were obtained for ankle and toe joint angles, which was anticipated due to their respectively lower tracker weightings. The GRFs of the model, more closely follow the more accurate GRF measurements from the subject (Fig. 4). It is evident, however, that the model leaves the ground nearly 20ms earlier than did the subject (Fig 4B, reaction is zero at 0.48s).

The joint torques (Fig. 5), corresponding to muscular moments computed by motion tracking, are consistent with the proximal to distal actuation pattern commonly observed in vertical jumping ([7], [11]) and are strikingly similar to the dynamic optimization solution obtained by parameter optimization [7] (Fig. 5, bold vs. thin lines).

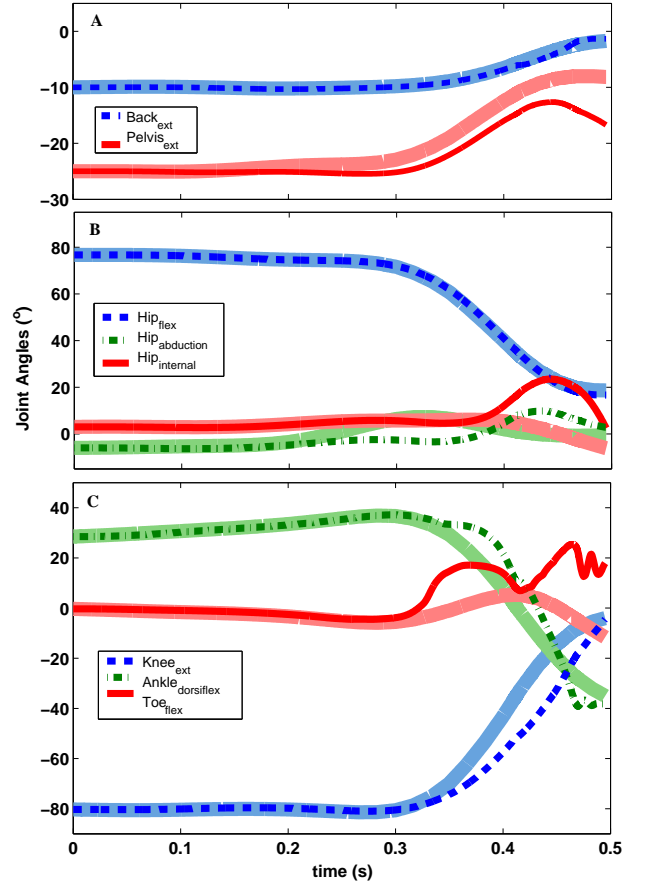


Figure 3. Simulated (bold) and experimental (shaded) joint angles for (A) the body (back and pelvis), (B) hip and (C) joints of the right leg.

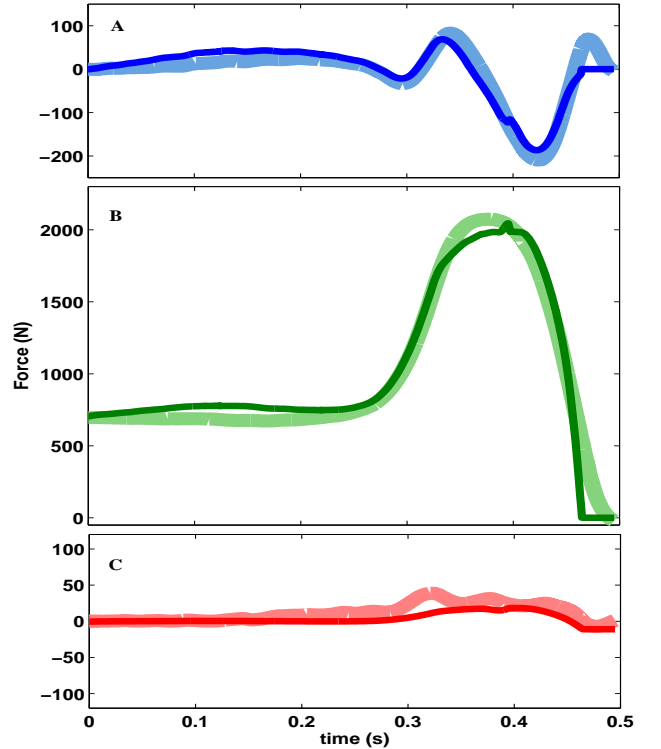


Figure 4. Simulated (bold) and experimental (shaded) GRFs. Net (A) fore-aft, (B) vertical and (C) medio-lateral forces.

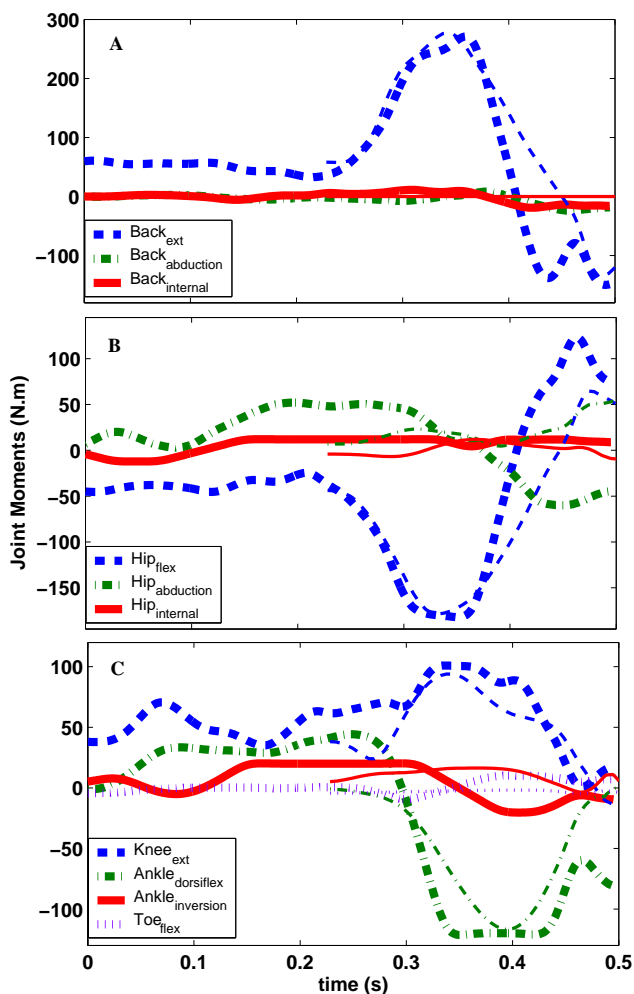


Figure 5. Motion tracking (bold) and parameter optimization [7] (thin) determinations of the applied joint moments. Computed joint moments of the (A) back (L4-L5) joint, (B) hip joint and (C) joints of the right leg. Note the parameter optimization solution was computed for a shorter time period and solutions were synchronized by take-off time for the purpose of comparison.

#### IV. DISCUSSION

Motion tracking was able to replicate the performance of a specific subject in forward dynamic simulation without using a large-scale optimization approach. In fact, comparable joint moments were obtained by motion-tracking in under 6 minutes versus the approximate 30 days (788 hours) of serial processing time required by parameter optimization [7]. The similarity of the tracking solution (of a single subject) with that predicted by the parameter optimization solution [7] (which used an average subject model) indicates that the predictive solution was indeed valid. On the other hand, it shows that dynamic optimization of a full musculoskeletal model is not necessary to determine the muscular moments that will reproduce observed human behavior. This is important from a clinical application perspective, where the underlying forces and moments are needed quickly (not in days or weeks) with models of high complexity. The tracking method also avoids some of the pitfalls of parameter optimization methods. Namely, initial guesses of the controls (discretized moment trajectories or individual muscle excitations) can be as difficult to obtain as the dynamic optimization solution itself.

In comparison, motion tracking does require some significant pre-processing prior to performing simulations. First, model parameters and initial moments must be determined such that the model matches the experimental data at time = 0s. The tracking method does not tolerate significant error upfront. Second, determining the set of weightings that produce good results over the performance period can be challenging. In our experience, intuition from data collection combined with trial and error is sufficient to obtain suitable weightings and is far less difficult than obtaining a viable initial guess to the parameter optimization algorithm. Furthermore, weightings tend to hold for a given model and motion-capture protocol. Therefore, we propose that the tracking approach be employed to systematically obtain initial solutions from which to predict future outcomes.

Because the motion-tracking method tries to match the behavior of a given model to experimental data, it is, by its very nature, a validation tool. Since it is relatively inexpensive to run tracking simulations, in contrast to parameter optimizations, models can be developed iteratively -gradually adding complexity to achieve the desired accuracy. In fact, this approach led us to improve the contact model and made it capable of producing similar inflections in the fore-aft component of the GRF.

#### ACKNOWLEDGMENT

The author is grateful for the guidance and support of Marcus G. Pandy (graduate advisor) and the financial support provided by the University of Texas and the Department of Biomedical Engineering; NASA; and the International Society of Biomechanics (ISB). Special thanks to the 3D Symposium organizing committee for making travel arrangements.

#### REFERENCES

- [1] R. D. Crowninshield and R. A. Brand. "A physiologically based criterion of muscle force prediction in locomotion," *J. Biomech.*, 14(11):793-801, 1981.
- [2] D. G. Thelen, F. C. Anderson, and S. L. Delp. "Generating dynamic simulations of movement using computed muscle control," *J. Biomech.*, 36:321-328, 2003.
- [3] D. G. Lloyd and T. F. Besier. "An emg-driven musculoskeletal model to estimate muscle forces and knee joint moments in vivo," *J. Biomech.*, 36:765-776, 2003.
- [4] D. W. Risher, L. M. Shutte, and C. F. Runge. "The use of inverse dynamics solutions in direct dynamics simulations," *J. Biomech. Eng.*, 119:417-422, 1997.
- [5] M. W. Spong and M. Vidyasagar. *Robot Dynamics and Control*. John Wiley Sons, Toronto, 1989.
- [6] A. Seth, J. J. McPhee, and M. G. Pandy. "Multi-joint coordination of vertical arm movement," *J. App. Bionics & Biomech*, 1(1):45-56, 2003.
- [7] F. C. Anderson and M. G. Pandy. "A dynamic optimization solution for vertical jumping in three dimensions," *CMBBE*, 2:201-231, 1999.
- [8] A. Seth and M. G. Pandy. "A neuromusculoskeletal tracking method for estimating individual muscle forces in human movement," *J. Biomech.*, in press.
- [9] J.-J. Slotine and W. Li. *Applied Nonlinear Control*. Prentice-Hall, Inc., New Jersey, 1991.
- [10] A. D. Kuo. "A least-squares estimation approach to improving the precision of inverse dynamics computations". *J. Biomech. Eng.*, 120, 148-159, 1998.
- [11] M. F. Bobbert and G. J. van Ingen-Schenau. "Coordination in vertical jumping". *J. Biomech.*, 21 (3), 249-262, 1988.

